Vilnius
University
Press

Soliton-like solutions supported by refined hydrodynamic-type model of an elastic medium with soft inclusions

Vsevolod Vladimirov[a], Sergii Skurativskyi[b]

[a]Faculty of Applied Mathematics,
AGH University of Science and Technology,
Al. Mickiewicza 30, Krakow, 30-059, Poland
vladimir@agh.edu.pl

[b]Subbotin Institute of Geophysics
  of the National Academy of Science of Ukraine,
Academician Palladin Ave., 32, Kyiv, 03680, Ukraine
skurserg@gmail.com

Abstract. A nonlinear elastic medium containing sharp inhomogeneities is considered. The properties of a modified model of such a medium are investigated. The modification consists in including in the asymptotic equation of state those terms that were discarded in the previously considered models. The main purpose of the ongoing research is to analyze the existence, stability, and dynamic properties of soliton-like solutions within the modified model, as well as to compare these solutions with analogous solutions obtained in the previously considered models.

Keywords: nonlocal media model, soliton-like solutions, stability, Evans function, simulation of solitary waves collision.

1 Introduction

This paper deals with a family of invariant traveling wave (TW) solutions of a hydro-dynamic-type model describing elastic media with internal structure. As it is shown in a number of papers (see e.g. [26–28] and references therein), the balance equations for mass and momentum in the long wave approximation retain their classical form, and the information about the presence of structure is manifested in the dynamical equation of state (DES), relating the pressure field to the field of density. In this study, we consider a model of a nonlinear elastic medium containing multiple evenly distributed inclusions (these can be cracks, cavities, or inclusions of a substance that differs significantly from the carrier material in its physical properties). In such a system, the density field at neighboring points can differ by orders of magnitude, which makes it appropriate to replace the functional dependence $p(t,x) = F[\rho(t,x)]$ between pressure and density

by the dependence of p on some averaged density. The integral relationship between the pressure and density is used in many papers (see [9, 19] and references therein). It is shown in [19] that if the nonlocal effects decay rapidly with distance, then the integral relation can be replaced by an approximate functional–differential relation, which is more beneficial in studying the system and, at the same time, leads to a qualitatively similar description. The authors of the work [19] replace the density function under the integral with the first few terms of its expansion in a Taylor series, after which it is possible to calculate the integral exactly. However, here the question arises as to how many terms of the series expansion should be taken into account. This kind of questions typically arises in models whose derivation includes the methods of asymptotic decomposition (remind, e.g. the construction of the KdV-type equations from the Fermi–Pasta–Ulam problem [8] and the study of this issue in more recent works [6, 7, 17]). In practice, the question of the number of retained terms of the asymptotic expansion is solved not least for reasons of convenience since a more "exact" model, as a rule, turns out to be too difficult to study. The hydrodynamic model of an elastic structured medium proposed in [19] (see also [20]) includes the minimal number of terms in the asymptotic expansion of the dynamic equation of state required to take into account nonlocal effects. This model is further investigated in papers [29, 30] in order to state the existence of soliton-like solutions (which, as is known, are absent in the classical hydrodynamic-type model), their stability, and dynamical features. The questions mentioned have found exhaustive solutions in the papers [29, 30] in which criteria for the existence of one-parameter families of soliton-like solutions are stated, which, depending on the values of the parameters, describe waves of compression or rarefaction, as well as stability issues. In these works, integrability tests were also carried out, which gave a negative result. Despite this, the system considered in [29, 30] possesses stable localized solutions manifesting some features of "pure" solitons to which we would like to pay special attention.

As in the vast majority of works devoted to the study of asymptotic models with soliton solutions, the question of how the discarded terms affect the existence of solitons and their stability remains open. But there is some evidence that, with certain modifications of the equation of state [17], as well as the incorporation of nonlocal effects [12], soliton structures are preserved, however, these changes radically affect the stability of localized solutions and their dynamic properties.

This work is devoted to clarifying the persistence of soliton solutions under natural modification of the model described in [29, 30] and to studying properties of localized solutions supported by the modified model. The structure of the article is the following. In Section 2, we pose the statement of the problem and review the previously obtained results concerning the conditions for the existence of soliton solutions and their stability. In Section 3, we give the numerical evidence of the existence of the solitary wave solutions supported by the refined model. In Section 4, we discuss a concept of spectral stability formulated in terms of the properties of the linearized operator built on the original system and study its essential spectrum. In Section 5, we construct the Evans function used further for the numerical study of the discrete (point) spectrum of the operator of linearization. Section 6 is devoted to the numerical study of the dynamic properties of soliton-like solutions. In Section 7, we briefly discuss the results obtained.

2 Statement the problem and review of the previously obtained results

Thus, we consider nonlinear elastic media containing cavities, microcracks, or soft inclusions. Description of nonlinear waves propagation in such media depends in essential way on the ratio of a characteristic size d of elements of medium structure to a characteristic length λ of the wave pack. If $d/\lambda = O(1)$, then the basic concepts of continuum mechanics are not applied, and one should use the description based, e.g. on the element dynamics methods. If, in turn, $d/\lambda \ll 1$, then one can use the equations of classical continuum mechanics, completely ignoring the presence of internal structure.

The model considered in this work applies when the ratio d/λ is much less than unity and the continual approach is valid, however, the physical characteristics of the material at adjacent points can differ abruptly from each other, and therefore the description that does not takes into account the internal structure of the medium is incorrect.

As it has been shown in [26], in the long wave approximation the balance equations for mass and momentum retain their classical form, which in the one-dimensional case can be written as follows:

$$u_t + p_x = 0, \qquad \rho_t + \rho^2\, u_x = 0, \tag{1}$$

where u is the velocity, p is the pressure, ρ is the density, t is the time, x is the mass (Lagrange) coordinate; subscripts denote partial derivatives with respect to subsequent variables.

When describing adiabatic processes occurring in an elastic nonlinear homogeneous medium, the local equation of state $p = A\rho^{\nu+2}$, $\nu > -1$, is most often used. However, if the medium is strongly inhomogeneous and the density field can change abruptly from point to point, it seems appropriate to relate the pressure field to the averaged density field using the integral equation

$$p(t, x) = \int\limits_{-\infty}^{+\infty} K(x, x')\, \rho^{\nu+2}(t, x')\, \mathrm{d}x', \tag{2}$$

where $K(x, x')$ is the kernel of nonlocality, which can be calculated in principle by solving the dynamical problem of structure elements interaction. However, such calculations are very difficult, and in practice, one uses as a rule some model kernels describing well enough main properties of the nonlocal effects and, in particular, the fact that these effects vanish rapidly as $|x - x'|$ grows. This condition is satisfied by the kernel of the following form:

$$K(x, x') = \Phi\big(|x - x'|\big) \exp\left[\frac{-(x - x')^2}{l^2}\right], \tag{3}$$

where $\Phi(z)$ is a polynomial of a finite order. Such a model is attributed in the papers [19, 20] with $\Phi(z) = A = \mathrm{const}$ to the elastic medium containing the low density inclusions. Using the fact that the function (3) extremely quickly approaches zero as

$|x - x'|$ grows, one can replace $\rho^{\nu+2}(t, x')$ in formula (2) by three terms of its power series decomposition around x:

$$
\begin{aligned}
\rho^{\nu+2}(t, x') = \rho^{\nu+2}(t, x') &+ \frac{x' - x}{1!}\big[\rho^{\nu+2}(t, x')\big]_x \\
&+ \frac{(x' - x)^2}{2!}\big[\rho^{\nu+2}(t, x')\big]_{xx} + O\big(|x' - x|^3\big),
\end{aligned}
$$

obtaining after the integration DES

$$
p = \frac{1}{\nu + 2}\left(\beta + \sigma\frac{\partial^2}{\partial x^2}\right)\rho^{\nu+2}(t, x'), \tag{4}
$$

where $\beta = Al\sqrt{\pi}(\nu + 2)$, $\sigma = Al^3(\nu + 2)\sqrt{\pi}/4$. Further, the authors of [19] show that the description of the dynamic properties of solutions supported by the model with the integral DES (2) is qualitatively the same as that of the model in which the relation (4) is used as a DES.

In papers [29, 30] in which the kernel

$$
K(x, x') = A\big[\mu + \alpha(x - x')^2\big]\exp\left[\frac{-(x - x')^2}{l^2}\right] \tag{5}
$$

is used, a DES of the form (4) is obtained with the coefficients $\beta = Al(\nu + 2)\sqrt{\pi} \times (2\mu + \alpha l^2)/2$, $\sigma = Al^3(\nu + 2)\sqrt{\pi}\mu/4$. It is easily seen that when $\mu < 0$ and $\alpha > -2\mu/l^2$, then β remains positive, while σ becomes negative. Note that a well-established linear strain–stress dependence corresponding to the above situation is presented in papers [3, 9] in which the model describing the propagation of waves in a crystal lattice taking into account the influence of dislocations is considered.

In deriving the refined DES closing the hydrodynamic system (1), we will still assume that the kernel function is described by formula (5) and simultaneously keep the terms up of the order $O(|x - x'|^4)$ in the decomposition of the function $\rho(t, x')$ in the Taylor series around x. After the integration, we get the following DES:

$$
p = \frac{1}{\nu + 2}\big(\beta + \sigma\partial_x^2 + \kappa\partial_x^4\big)\rho^{\nu+2}, \tag{6}
$$

where $\beta = Al(\nu + 2)\sqrt{\pi}(l^2\alpha + 2\mu)/2$, $\sigma = Al^3(\nu + 2)\sqrt{\pi}(2\mu + 3l^2\alpha)/8$, $\kappa = A\mu l^5(\nu + 2)\sqrt{\pi}/32$. Obviously, the signs of the above parameters depend on the signs of the coefficients μ and α. In what follows, we will be interested in the case when β and κ are positive, while σ can be both positive and negative. Note that σ is negative, while the remaining parameters are positive, if $\mu > 0$, $\alpha < 0$, and the following inequalities hold: $-\alpha l^2/2 < \mu < -3\alpha l^2/2$.

So, the employment of the model kernel (5) enables to vary the sign of the parameter σ in the DES (6). Note, however, that the case $\sigma > 0$ can be obtained within the approach presented in [20] just by keeping terms of the order $O(|x - x'|^4)$ in the Taylor expansion of the integrand. For $\sigma < 0$, a DES similar to (6) was obtained in the linear case in paper [9].

In papers [9,20] the substantiation of the models used and their comparison with empirical results are given. The DES obtained in [9] can be generalized to the nonlinear case, posing the condition of the preliminary stress of the medium and moving away from the Hookean stress–strain dependence.

Now, let us briefly describe the results obtained for the system

$$u_t + \frac{1}{\nu + 2}\big(\beta + \sigma\partial_x^2\big)\partial_x\rho^{\nu+2} = 0, \tag{7}$$

$$\rho_t + \rho^2 u_x = 0 \tag{8}$$

extracted from (1) by replacement of p with the DES (4). System (7)–(8) is considered in [29, 30], where the existence of solutions of the form

$$u = U(\xi), \qquad \rho = R(\xi), \qquad \xi = x - st \tag{9}$$

describing solitary waves is shown, and the stability of these solutions is studied in detail. The results obtained in this paper can be summarized as follows.

- If $\beta > 0$, $\sigma < 0$, and the inequalities

$$\frac{\beta(\nu + 1)}{2(\nu + 2)} R_1^{\nu+3} < s^2 < \beta R_1^{\nu+3}, \tag{10}$$

$$0 < R_1 = \lim_{|\xi| \to +\infty} R(\xi) \tag{11}$$

  are satisfied, then there exist solutions describing the solitary waves of rarefaction.
- If, in turn, $\beta > 0$, $\sigma > 0$, and the inequality

$$s^2 > \beta R_1^{\nu+3} \tag{12}$$

  is satisfied, then there exist solutions describing the solitary waves of compression.
- The solitary waves of rarefaction are spectrally stable under certain conditions, while the solitary waves of compression are always unstable.

In the following, we will consider the system

$$u_t + \frac{1}{\nu + 2}\big(\beta + \sigma\partial_x^2 + \kappa\partial_x^4\big)\partial_x\rho^{\nu+2} = 0, \tag{13}$$

$$\rho_t + \rho^2 u_x = 0 \tag{14}$$

obtained by substituting the modified state equation (6) into system (1), mainly concentrating on stating the existence of the soliton-like TW solutions and studying how does the addition of terms with higher derivatives affects the stability of soliton profiles and their dynamical features. Note that in what follows, we will also keep conditions (10), (11), and (12), which guarantee the presence of solitary waves in the limiting case $\kappa = 0$. Note also that for $\sigma < 0$, conditions (10) and (11) act as a necessary conditions for the existence of soliton-like solutions [24].

3 Qualitative and numerical study of the existence of solitary wave solutions in model (13)–(14)

We are looking for the solitary wave solutions belonging to the set of functions (9). We assume in addition that the solutions obey the asymptotics conditions

$$\lim_{|\xi|\to+\infty} U(\xi) = 0, \qquad \lim_{|\xi|\to+\infty} R(\xi) = R_1 > 0.$$

Inserting the ansatz (9) into Eq. (14) and integrating the ODE obtained this way within the interval $(-\infty, \xi)$, we get the quadrature

$$U(\xi) = s\left(\frac{1}{R_1} - \frac{1}{R(\xi)}\right).$$

Inserting then the TW ansatz into Eq. (13) and using the above quadrature for the elimination of $U(\xi)$, we obtain, after one integration, the equation

$$s^2\left(\frac{1}{R(\xi)} - \frac{1}{R_1}\right) + \frac{\beta}{\nu+2}\left(R^{\nu+2} - R_1^{\nu+2}\right)$$
$$+ \frac{1}{\nu+2}\left(\sigma\frac{d^2}{d\xi^2} + \kappa\frac{d^4}{d\xi^4}\right)R^{\nu+2} = 0. \tag{15}$$

We present Eq. (15) in the form of an equivalent dynamical system:

$$\begin{pmatrix} R \\ V \\ W \\ P \end{pmatrix}' = \begin{pmatrix} V \\ W \\ P \\ -\Psi(R,V,W,P)/(\kappa R^{\nu+1}) \end{pmatrix}, \tag{16}$$

where

$$\Psi(R,V,W,P) = (\nu+1)\kappa\big[R^\nu\big(4VP + 3R^\nu W^2\big)$$
$$+ 6\nu R^{\nu-1}V^2 W + \nu(\nu-1)R^{\nu-2}V^4\big]$$
$$+ \sigma\big[R^{\nu+1}W + (\nu+1)R^\nu V^2\big] + \Phi(R),$$
$$\Phi(R) = \frac{\beta}{\nu+2}\left(R^{\nu+2} - R_1^{\nu+2}\right) + s^2\left(\frac{1}{R} - \frac{1}{R_1}\right).$$

The coordinates of the stationary points of the dynamical system are determined by the relations $V = W = P = \Phi(R) = 0$. The only nonzero coordinate R satisfies the equation $\Phi(R) = 0$ having one evident solution $R = R_1$. Since we are interested in localized TW solutions satisfying the asymptotics $\lim_{\xi\to\pm\infty} R = R_1$, the stationary point $P = (R_1, 0, 0, 0)$ should have the character of a saddle point, in other words, it must have both ongoing and outgoing separatrices. Let us analyze under what conditions this is possible. To this end, we consider the linearization of the system at the stationary point P.

Introducing the coordinate $X = R - R_1$ and discarding the nonlinear terms in (16), we obtain the system

$$
\begin{pmatrix} X \\ V \\ W \\ P \end{pmatrix}' = \begin{pmatrix} 0 & 1 & 0 & 0 \\ 0 & 0 & 1 & 0 \\ 0 & 0 & 0 & 1 \\ -A & 0 & -B & 0 \end{pmatrix} \begin{pmatrix} X \\ V \\ W \\ P \end{pmatrix} = \widehat{M} \begin{pmatrix} X \\ V \\ W \\ P \end{pmatrix},
$$

where $A = (\beta R_1^{\nu+3} - s^2)/(\kappa R_1^{\nu+3})$, $B = \sigma/\kappa$. The eigenvalues of the matrix $\widehat{M}$ can be obtained by solving the characteristic equation

$$
\lambda^4 + \lambda^2 B + A = 0.
$$

It is evident that the parameter $\theta = \lambda^2$, satisfying the corresponding quadratic equation, attains the following values:

$$
\theta_\pm = \frac{-B \pm \sqrt{\Omega}}{2}, \qquad \Omega = \left(\frac{\sigma}{\kappa}\right)^2 - \frac{4}{\kappa R_1^{\nu+3}}\left(\beta R_1^{\nu+3} - s^2\right).
$$

So, the matrix $\widehat{M}$ will have a pair of real roots of different signs (this condition ensures that the stationary point P has incoming and outgoing separatrices) if at least one of the roots $\theta_\pm$ is positive. Let us analyze such possibilities keeping inequalities (12) and (10)–(11) for the cases of $\sigma > 0$ and $\sigma < 0$, respectively.

1. Case $\sigma > 0$ and $s^2 > \beta R_1^{\nu+3}$. For such restrictions $\Omega > (\sigma/\kappa)^2$, so $\theta_+ > 0$, while $\theta_- < 0$. Since the matrix $\widehat{M}$ has a pair of real roots of different signs and a pair of purely imaginary roots, the stationary point P is a saddle-center.

2. Case $\sigma < 0$ and $s^2 < \beta R_1^{\nu+3}$. Under the specified restrictions and the fulfillment of the additional condition

$$
\frac{\sigma^2}{\kappa} > \frac{4\kappa}{R_1^{\nu+3}}\left(\beta R_1^{\nu+3} - s^2\right),
$$

both θ_+ and θ_- are positive. Therefore, all the eigenvalues of the matrix $\widehat{M}$ are real, half of them positive, and the stationary point P is a saddle.

Thus, in both cases, when the corresponding inequalities are satisfied, the stationary point P possesses both ongoing and outgoing separatrices, which, in principle, can form homoclinic loop. If such a trajectory does exist, it can be caught numerically by solving initial value problem, with the initial data choosing sufficiently close to the stationary point P, and lying on the line defined by the eigenvector $(1, \lambda, \lambda^2, \lambda^3)$, where λ is a positive eigenvalue of the matrix $\widehat{M}$. The results of numerical experiments are shown in Figs. 1, 2, which represent both the homoclinic trajectories and the corresponding soliton-like solutions of the initial system (13)–(14).
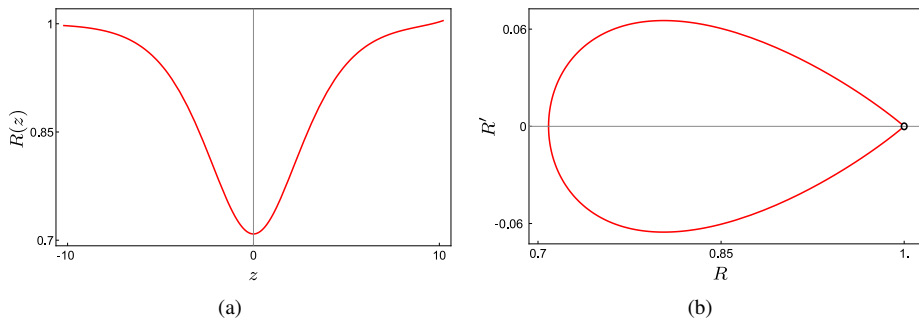
Figure 1. Profile of the solitary wave (a) and the projection of the corresponding homoclinic solution onto the R,R'-plane (b) obtained for the following values of the parameters: $\nu = 0$, $R_1 = 1$, $\beta = 2$, $s = 1.2$, $\sigma = -1.8$, $\kappa = 1.2$.
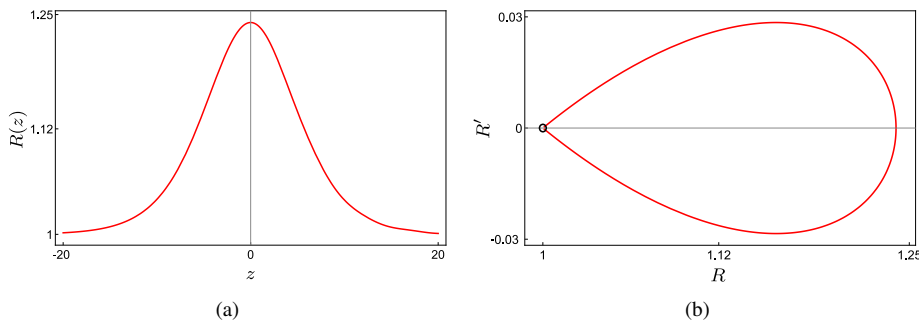
Figure 2. Profile of the solitary wave (a) and the projection of the corresponding homoclinic solution onto the R,R'-plane (b) obtained for the following values of the parameters: $\nu = 0$, $R_1 = 1$, $\beta = 0.8$, $s = 1$, $\sigma = 1.8$, $\kappa = 1.25$.

Remark 1. In the case when the stationary point P is a saddle-center, it is very difficult to obtain the homoclinic trajectory by the direct numerical integration because the incoming trajectory is extremely unstable. Therefore, in order to obtain the homoclinic loop presented in Fig. 2, we used a combined method. First, we obtained numerically a half-trajectory moving along the outgoing separatrix until the value ξ_0 at which the function $R(\xi)$ reached its maximum. The remaining part of the trajectory was obtained using the parity of the function $R(\xi)$ resulting from the invariance of Eq. (15) with respect to the change of the independent variable $\xi \to -\xi$.

Remark 2. We restricted ourselves to analyzing the eigenvalues of the matrix $\widehat{M}$ only for the cases listed above, omitting two other cases, namely,

$$(\sigma > 0) \wedge \left(s^2 > \beta R_1^{\nu+3} \right) \quad \text{and} \quad (\sigma < 0) \wedge \left(s^2 < \beta R_1^{\nu+3} \right)$$

for the reason that conditions (10), (11) in the case when $\sigma < 0$ and, most likely, condition (12) in the case when $\sigma > 0$ serve as necessary conditions for the existence of the trajectories biasymptotic to the stationary point P [24].

4   Spectral stability of the soliton-like solutions

In the study of spectral stability of TW solutions, it is helpful to pass to new independent variables $\bar{t} = t$, $\bar{\xi} = x - st$ in which the invariant TW solutions (9) become stationary. In the new variables, system (13)–(14) reads as follows:

$$u_{\bar{t}} - su_{\bar{\xi}} + \frac{1}{\nu + 2}\mathcal{L}\partial_{\bar{\xi}}\rho^{\nu+2} = 0, \qquad \rho_{\bar{t}} - s\rho_{\bar{\xi}} + \rho^2 u_{\bar{\xi}} = 0, \qquad (17)$$

where $\mathcal{L} = \beta + \sigma\partial_{\bar{\xi}}^2 + \kappa\partial_{\bar{\xi}}^4$. For the sake of simplicity, the bars will be omitted from now on. We restrict ourselves to the analysis of spectral stability [10,11,16,23] of the TW solution $[U(\xi), R(\xi)]^{\mathrm{tr}}$ and consider the perturbations of the following form:

$$u(t, \xi) = U(\xi) + \epsilon\exp[\lambda t]f(\xi), \qquad \rho(t, \xi) = R(\xi) + \epsilon\exp[\lambda t]g(\xi), \qquad (18)$$

where λ is the spectral parameter, and $|\epsilon| \ll 1$.

Inserting the ansatz (18) into system (17) and neglecting the terms of the order $O(|\epsilon|^2)$, we obtain the system linearized about the traveling wave solutions:

$$f\lambda - sf' + \mathcal{L}\left[R^{\nu+1}g\right]' = 0, \qquad R^2 f' - sg' + g(\lambda + 2RU') = 0, \qquad (19)$$

where the primes denote derivatives with respect to ξ.

It is obvious that system (19) can be treated as a spectral problem

$$Ly = \lambda y, \quad y = (f, g)^{\mathrm{tr}} \qquad (20)$$

for the operator

$$L = \begin{pmatrix} s\partial_\xi, & -\mathcal{L}\{[R^{\nu+1}]' + R^{\nu+1}\partial_\xi\} \\ -R^2\partial_\xi, & s\partial_\xi - 2RU' \end{pmatrix}. \qquad (21)$$

Recall that the set of all possible values of $\lambda \in \mathbb{C}$ for which equation (20) has nontrivial solutions is called the spectrum Σ of the operator L. The homoclinic solution $[U(\xi), R(\xi)]^{\mathrm{tr}}$ is said to be spectrally stable if no possible eigenvalue λ belongs to the right half-plane of the complex plane [16].

As usually, we distinguish the essential spectrum $\Sigma_{\mathrm{ess}} \subset \Sigma$ and the discrete spectrum $\Sigma_{\mathrm{discr}} \subset \Sigma$. Being somewhat informal, we can interpret Σ_{ess} and Σ_{discr} as the subsets responsible, respectively, for the stability of the asymptotic stationary solution $(0, R_1)$ and the solution $[U(\xi), R(\xi)]^{\mathrm{tr}}$ itself.

Now we are going to state the conditions, which guarantee that the set $\Sigma_{\mathrm{ess}} \cap \mathbb{C}^+$ is empty. In the limiting case $|\xi| \to \pm\infty$, the variational system turns into the linear system with constant coefficients

$$\lambda f = sf' - \mathcal{L}R_1^{\nu+1}g', \qquad \lambda g = sg' - R_1^2 f'. \qquad (22)$$

Location of the essential spectrum can be determined using the Fourier transform. Applying the latter to system (22), we get

$$\widehat{M}(\eta, \lambda)\begin{pmatrix} \hat{f}(\eta) \\ \hat{g}(\eta) \end{pmatrix} = \begin{pmatrix} \lambda + \mathrm{i}\eta s, & -\mathrm{i}\eta R_1^{\nu+1}\hat{\mathcal{L}}(\eta) \\ -\mathrm{i}\eta R_1^2, & \lambda + \mathrm{i}\eta s \end{pmatrix}\begin{pmatrix} \hat{f}(\eta) \\ \hat{g}(\eta) \end{pmatrix} = 0, \qquad (23)$$

where $\hat{f}(\eta)$ and $\hat{g}(\eta)$ are the Fourier transforms of $f(\xi)$ and $g(\xi)$, respectively,

$$\hat{\mathcal{L}}(\eta) = \beta - \sigma\eta^2 + \kappa\eta^4.$$

Equating $\det \widehat{M}(\eta, \lambda)$ to zero, we obtain the expression for eigenvalues

$$\lambda_{1,2} = -\mathrm{i}\eta s \pm \mathrm{i}\eta R_1^{(\nu+3)/2}\sqrt{\beta - \sigma\eta^2 + \kappa\eta^4}, \quad \eta \in \mathbb{R}.$$

Thus, the following assertion holds.

Statement. *If $\hat{\mathcal{L}}(\eta) > 0$ for all $\eta \in \mathbb{R}$, then Σ_{ess} is located on the imaginary axis. Otherwise, $\Sigma_{\mathrm{ess}} \cap \mathbb{C}^+ \neq \emptyset$.*

Let us now analyze what restrictions the condition

$$\beta - \sigma\eta^2 + \kappa\eta^4 > 0, \quad \eta \in \mathbb{R}, \tag{24}$$

poses on the coefficients. First of all, we note that the fulfillment of condition (24) is impossible when $\kappa < 0$ and that is the reason on why we have restricted our consideration to the case $\kappa > 0$.

In case of the positive κ, fulfillment of condition (24) is possible if all the roots of the equation

$$\beta - \sigma\eta^2 + \kappa\eta^4 = 0 \tag{25}$$

have nonzero imaginary parts. Analyzing the roots

$$\eta = \pm\sqrt{\frac{\sigma \pm \sqrt{\Delta}}{2\kappa}}, \quad \Delta = \sigma^2 - 4\beta\kappa$$

of the biquadratic equation (25), the following subcases can be distinguished:

1. $\sigma > 0$, $\Delta < 0$;
2. $\sigma < 0$, Δ is arbitrary.

For these cases, it makes sense to study the location of the points of the discrete spectrum.

5 Study of the discrete spectrum

We shall study the discrete spectrum of the operator (21) by means of the Evans function technique [10, 11], which is widely used in studying discrete spectra of linear operators with variable coefficients. To construct the Evans function for the case under consideration, some preliminary calculations should be performed. At first, using the new variables

$$Rg = v, \qquad \kappa Z = sf - \beta v - \sigma v'' - \kappa v'''',$$

the linearized system (19) can be transformed for the case $\nu = 0$ into the following system of first-order equations:

$$
Y' = \begin{pmatrix} f \\ v \\ Z_1 \\ Z_2 \\ Z_3 \\ Z \end{pmatrix}' = \begin{pmatrix} 0 & -(\lambda+2U'R+sR'/R)/R^3 & s/R^3 & 0 & 0 & 0 \\ 0 & 0 & 1 & 0 & 0 & 0 \\ 0 & 0 & 0 & 1 & 0 & 0 \\ 0 & 0 & 0 & 0 & 1 & 0 \\ s/\kappa & -\beta/\kappa & 0 & -\sigma/\kappa & 0 & -1 \\ \lambda/\kappa & 0 & 0 & 0 & 0 & 0 \end{pmatrix} \begin{pmatrix} f \\ v \\ Z_1 \\ Z_2 \\ Z_3 \\ Z \end{pmatrix}
$$

$$ = AY. \tag{26} $$

Due to the asymptotic behavior of solitary waves, the matrix A attains the same form at $\pm\infty$, which is as follows:

$$
A^\infty = \begin{pmatrix} 0 & -\lambda/R_1^3 & s/R_1^3 & 0 & 0 & 0 \\ 0 & 0 & 1 & 0 & 0 & 0 \\ 0 & 0 & 0 & 1 & 0 & 0 \\ 0 & 0 & 0 & 0 & 1 & 0 \\ s/\kappa & -\beta/\kappa & 0 & -\sigma/\kappa & 0 & -1 \\ \lambda/\kappa & 0 & 0 & 0 & 0 & 0 \end{pmatrix}.
$$

Since there are many publications devoted to the Evans function method, there is no point in describing it in detail. We only note that the main idea of this method is the study of intersections of sets $W_\lambda^\pm(\xi)$, where $W_\lambda^-(\xi)$ denotes the manifold spanned on the solutions of (26) that decay as $x \to -\infty$, while $W_\lambda^+(\xi)$ denotes the manifold spanned on the solutions of (26) that decay as $x \to +\infty$. And if for some λ_0, $W_{\lambda_0}^-(\xi) \cap W_{\lambda_0}^+(\xi) \neq \emptyset$, then $\lambda_0 \in \Sigma_{\mathrm{discr}}$. Note also that the function proposed by Evans in the works [10, 11] is an analytic function of the parameter λ that nullifies at the points of the discrete spectrum of the corresponding linear operator.

The way of the Evans function evaluation depends on the structure of stable and unstable manifolds for system (26) at infinity. In turn, the dimensions of these manifolds are defined by the spectrum of the matrix A^∞, which can be evaluated from the corresponding characteristic polynomial

$$ \det\|A^\infty - \mu I\| = (\lambda - s\mu)^2 - R_1^3\mu^2\big(\beta - \sigma\mu^2 + \kappa\mu^4\big) = 0. \tag{27} $$

Equation (27) possesses six roots representing the matrix eigenvalues. When the eigenvalue μ is not multiple, the corresponding eigenvector is

$$ \vec{Y}_\mu = \left(\frac{s\mu - \lambda}{\mu R_1^3}; 1; \mu; \mu^2; \mu^3; \lambda\frac{s\mu - \lambda}{\kappa\mu^2 R_1^3} \right). $$

In our case, the spectrum consists of three eigenvalues with positive real parts and the same number of eigenvalues with the negative real parts. Thus, in order to get the bounded solutions of system (26) vanishing at infinity, the intersections of three dimensional manifolds should be gained.

To do this, we use the approach involving exterior algebra [2,5]. Thus, we consider the dynamics of system (26) on the wedge vector space $\wedge^3(\mathbb{C}^6)$ (with standard basis) in which three linearly independent vectors can be represented as a point [1], i.e. it is the space of all three-forms on $\mathbb{C}^6$. Then the induced system reads as follows: $\vec{Z}' = A^{(3)}\vec{Z}, \vec{Z} \in \mathbb{C}^{20}$, where the explicit form of the matrix $A^{(3)}$ can be found in [1, p. 256, App.] or [14, App. A]. As is well known [2], the eigenvalues of limiting matrix $(A^\infty)^{(3)}$ coincide with all possible sums of eigenvalues of the matrix A^∞. Thus, the eigenvalue of $(A^\infty)^{(3)}$ with smallest real part is the sum of all eigenvalues of A^∞ with negative real parts, while the eigenvalue of $(A^\infty)^{(3)}$ with the largest real part is the sum of all eigenvalues of A^∞ with positive real parts. Using the definition of three-form construction and expression for $\vec{Y}_\mu$, the explicit forms of corresponding eigenvectors $\vec{Z}^{\pm\infty}$ of $(A^\infty)^{(3)}$ can be written.

To construct the Evans function [1, 4, 5, 13–15, 18], we integrate the induced system over the interval $[0, L]$, where L represents the numerical infinity, starting from the eigenvector $\vec{Z}^{+\infty}$ at $\vec{Z}(L)$, and over the interval $[-L, 0]$ starting from the eigenvector $\vec{Z}^{-\infty}$ at $\vec{Z}(-L)$. Then, taking the resulting solutions $\vec{Z}^+(\xi)$ and $\vec{Z}^-(\xi)$ and evaluating their values at the point $\xi = 0$, we can construct the Evans function, which is defined as follows:

$$Ev(\lambda) = \vec{Z}^-(0)^{\mathrm{tr}} \cdot \widehat{\Sigma} \cdot \vec{Z}^+(0),$$

where $\widehat{\Sigma}$ is the skew-symmetric antidiagonal matrix [2, 14] with the following nonzero entries $\widehat{\Sigma}_{i, 21-i} = -1$ for $i = 2, 4, 6, 9, 12, 15, 17, 19$ and $\widehat{\Sigma}_{i,21-i} = 1$ for other diagonal elements.

Next, we evaluate the Evans function for the specified parameter values and consider two cases (for both cases $\nu = 0$ and $R_1 = 1$).

Case 1. The parameter values are as follows:

$$\beta = 2, \qquad s = 1.2, \qquad \sigma = -1.8, \qquad \kappa = 1.2.$$

Choosing the parameters as above, we get the subcase 2 mentioned at the end of the previous section, namely, $\sigma < 0$ and $\Delta = -6.36 < 0$. First, we take the solitary wave shown in Fig. 1. The shape of the curve tells us that this wave can be referred as a rarefaction wave. Applying the procedure of the Evans function evaluation outlined above, the graph of $Ev(\lambda)$ vs. real λ is obtained and is shown in Fig. 3(a). Since the curve does not intersect the horizontal axis, we can state that there are no positive real eigenvalues belonging to Σ_{discr}. In order to study the presence of complex discrete eigenvalues in the right half-plane, we use the Nyquist diagram technique. The values of the Evans function are derived along the closed contour lying in the right half-plane. Conventionally, the contour in the form of a semicircle is used, i.e. $\lambda = d + re^{i\theta}$. The typical Nyquist diagram is presented in Fig. 3(b). The contour becomes more complicated when the radius of circle r increases, yet the curve still does not enclose the origin, i.e. the winding number is zero. Thus, the eigenvalues with positive real parts inside the considered regions of the right half-plane were not found in numerical experiments, and the solitary wave of rarefaction can be considered as spectrally stable.
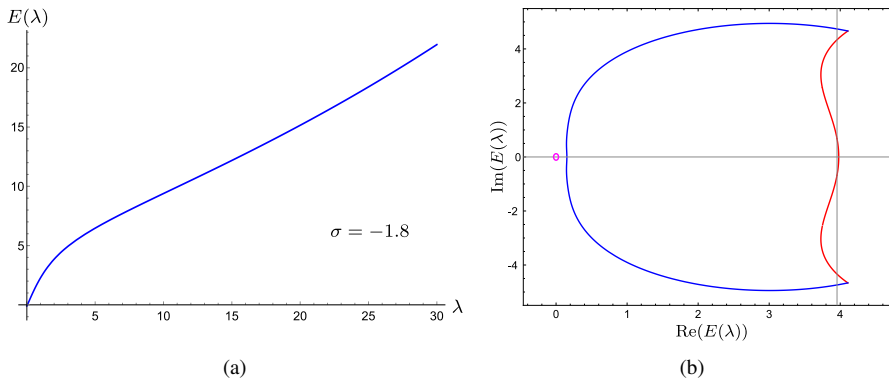
Figure 3. Evans function outputs for real values of λ (a) and for semicircular contour $\lambda = d + re^{i\theta}$, $d = 0.1$, $r = 2$ (b), evaluated at the following values of the parameters: $\beta = 2$, $s = 1.2$, $\sigma = -1.8$, $\kappa = 1.2$.
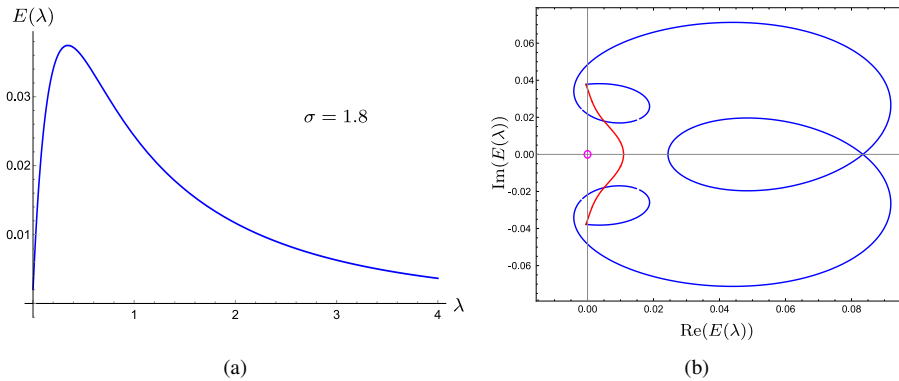
Figure 4. Evans function outputs for real values of λ (a) and for semicircular contour $\lambda = d + re^{i\theta}$, $d = 0.1$, $r = 2$ (b), evaluated at the following values of the parameters: $\beta = 0.8$, $s = 1$, $\sigma = 1.8$, $\kappa = 1.25$.

Case 2. The fixed parameter values are as follows:

$$\beta = 0.8, \qquad s = 1, \qquad \sigma = 1.8, \qquad \kappa = 1.25.$$

This is subcase 1 corresponding to $\sigma > 0$ and $\Delta < 0$ (see the classification given at the end of the previous section). The profile of the solitary wave and the projection of the phase trajectory of Eq. (15) on the R,R'-plane are plotted in Fig. 2, correspondingly. In contrast to the previous case, the solitary wave represents the wave of compression. The real-valued Evans function is presented in Fig. 4(a), whereas the Evans function output along the closed contour $\lambda = d + re^{i\theta}$, where $d = 0.1$ and $r = 2$, is plotted in Fig. 4(b). From these it follows that there are no discrete eigenvalues with positive real part in the corresponding regions of the positive half-plane of the complex plane, and, like in the previous case, the solitary wave of compression can be considered as spectrally stable.

6 Numerical simulations of dynamical behavior of the soliton-like solutions

To check the results of above analysis concerning the wave stability, the simulations of interaction of a pair of solitary waves are performed. To do this, we apply the proper numerical schemes for system (13)–(14) written in somewhat different form, namely,

$$
\frac{\partial u}{\partial t} + \frac{\partial p}{\partial x} = 0, \qquad \frac{\partial r}{\partial t} = u, \qquad \frac{\partial}{\partial t}\left(\frac{1}{\rho}\right) - \frac{\partial u}{\partial x} = 0, \tag{28}
$$

$$
p = \frac{\beta}{2}\rho^2 + \frac{\sigma}{2}\left(\rho^2\right)_{xx} + \frac{\kappa}{2}\left(\rho^2\right)_{xxxx},
$$

where $r(t)$ is the trajectory of a medium element.

The numerical scheme for system (28) is based on the integro–interpolating method [22] in which the approximation of the integral conservation laws is used. Note that, instead of the second equation of system (1), it is more convenient to use the following equation describing the volume element changing [22]:

$$
\frac{\partial r}{\partial x} = \frac{1}{\rho} - \frac{1}{R_1}.
$$

Within the framework of this approach, the following fully conservative numerical scheme is derived:

$$
\begin{aligned}
\frac{u_i^{j+1} - u_i^j}{\tau} &= -\frac{\gamma}{h}\left(p_i^{j+1} - p_{i-1}^{j+1}\right) - \frac{1-\gamma}{h}\left(p_i^j - p_{i-1}^j\right), \\
\frac{r_i^{j+1} - r_i^j}{\tau} &= \frac{u_i^{j+1} + u_i^j}{2}, \qquad r_{i+1}^{j+1} - r_i^{j+1} = \frac{h}{\rho_i^{j+1}} - \frac{h}{R_1}, \\
p_i^{j+1} &= \frac{\beta}{2}(\rho_i^{j+1})^2 + \frac{\sigma}{2}\frac{(\rho_{i-1}^{j+1})^2 - 2(\rho_i^{j+1})^2 + (\rho_{i+1}^{j+1})^2}{h^2} \\
&\quad + \frac{\kappa}{2}\frac{(\rho_{i-2}^{j+1})^2 - 4(\rho_{i-1}^{j+1})^2 + 6(\rho_i^{j+1})^2 - 4(\rho_{i+1}^{j+1})^2 + (\rho_{i+2}^{j+1})^2}{h^4},
\end{aligned} \tag{29}
$$

where $i = 3, \ldots, N - 2$. Here $\gamma = 0.5$, h and τ are spatial and temporal steps, respectively. From this scheme the quantities u_i^{j+1} and r_i^{j+1} can be excluded. Then we reduce relations (29) to the system with respect to p_i^{j+1} and ρ_i^{j+1}.

Using scheme (29), the evolution of a single solitary wave and collision of two identical waves moving toward each other are studied. The solutions of the latter problem are presented in Figs. 5 and 6 for cases 1 and 2, respectively. Analysis of the figures testifies that each solitary wave moves in self-similar mode. Moreover, the interaction, which is very similar to elastic (especially, in case 2), is revealed. The similar results are obtained also when there are used other numerical schemes, in particular, the scheme based on the Galerkin approximation. Thus, the numerical simulations confirm the conclusions of theoretical treatment concerning the stability of localized traveling wave solutions.

(a)   (b)
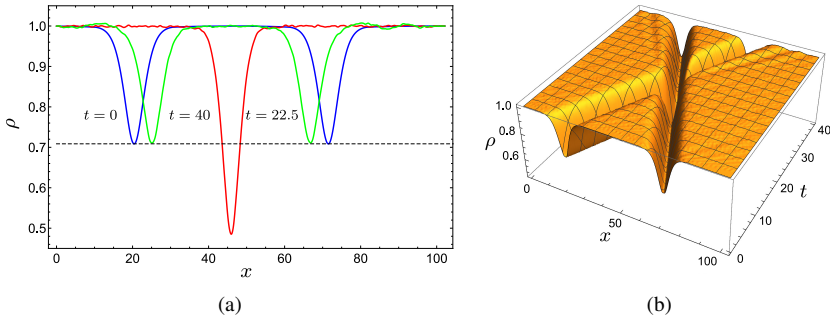
Figure 5. Collision of the solitary waves for the parameters corresponding to case 1. Panel (a) shows three profiles derived at $t = 0$ (blue curve), $t = 22.5$ (red curve), and $t = 40$ (green curve) time units. Panel (b) represents the 3D graph of wave interaction. Scheme parameters are as follows: $h = 0.0408$, $\tau = 0.05$, and $N = 2500$.

(a)   (b)
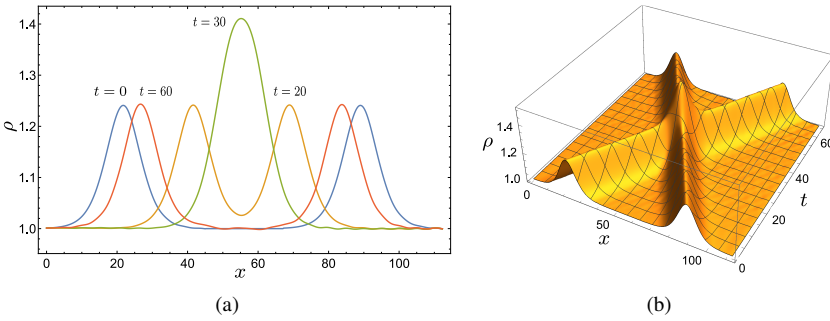
Figure 6. Collision of the solitary waves for the parameters corresponding to the case 2. Panel (a) shows four profiles derived at $t = 0$ (blue curve), $t = 20$ (brown curve), $t = 30$ (green curve), and $t = 60$ (red curve) time units. Panel (b) represents the 3D graph of wave interaction. Scheme parameters are as follows: $h = 0.225$, $\tau = 0.05$, and $N = 500$.

Another interesting and important problem concerning the solitary wave dynamics is the tracking of temporal evolution of an arbitrary wave disturbance. As an initial data we take a function different from the solitary wave solution. Since model (28) contains the higher derivatives, we should take a sufficiently smooth initial profile. The following initial density profile is used in the numerical experiments:

$$\rho = \begin{cases} a((x - x_0)^2 - y_0^2)^4 + R_1 & \text{if } |x - x_0| < y_0, \\ R_1 & \text{otherwise.} \end{cases} \tag{30}$$

The profile corresponding to $a = 3.6 \cdot 10^{-14}$, $x_0 = 40$, and $y_0 = 50$ is shown in Fig. 7(a). For comparison, the profile of the solitary wave from Fig. 2(a) is also shown on this graph.

Basing on formula (30), we construct the initial data for the pressure field using the following formula:

$$p = \frac{\beta}{2}\rho^2 + \sigma\big(\rho_x^2 + \rho\rho_{xx}\big) + \kappa\big(3\rho_{xx}^2 + 4\rho_x\rho_{xxx} + \rho F(\rho, \rho_x, \rho_{xx}, \rho_{xxx})\big),$$
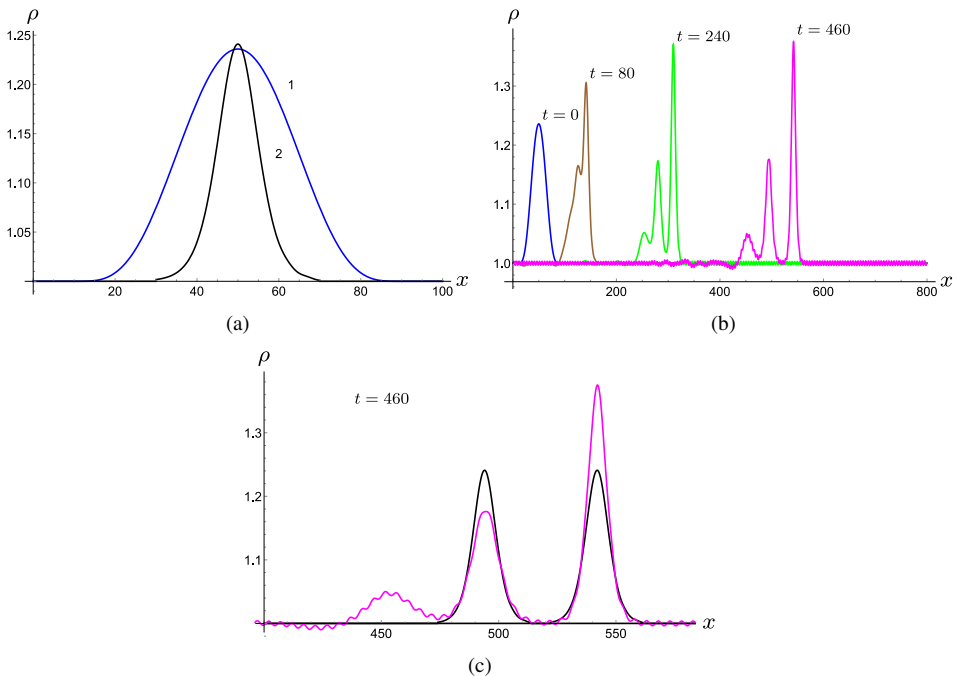
Figure 7. Splitting of the disturbance (30) into the train of solitary waves. Panel (a) shows initial density profile (30) (curve 1) and solitary wave from Fig. 2(a) (curve 2). Panel (b) represents solutions' profiles derived at $t = 0$ (blue curve coinciding with curve 1 in panel (a)), $t = 80$ (brown curve), $t = 240$ (green curve), and $t = 460$ (magenta curve). Panel (c) shows the enlargement of the solitary train profile taken at $t = 460$ (magenta curve), and doubly repeated curve 2 from the panel (a) shown for comparison (black curve).

where

$$F = (\kappa\rho)^{-1}\big(s^2\big(R_1^{-1} - \rho^{-1}\big) + 0.5\beta\big(R_1^2 - \rho^2\big) - \sigma\big(\rho_x^2 + \rho\rho_{xx}\big)$$
$$- \kappa\big(3\rho_{xx}^2 + 4\rho_x\rho_{xxx}\big)\big).$$

The scheme parameters are $N = 4000$ points, $L = 800$, space step $h = L/N$, temporal step $\tau = 0.2$. Integration of scheme (29) over the $2300\tau = 460$ time units results in wave dynamics shown in Fig. 7(b). Analysis of this figure shows the development of a train of solitary waves. Comparing the profiles of humps formed at $t = 460$ with the solitary wave profile (Fig. 7(c)), we see the equality of their widths.

7 Conclusions

So, the paper considers a modified model of a structured media proposed in [20, 29]. The modification consists in incorporating an extra term into the Taylor decomposition used when deriving the dynamic equation of state connecting the pressure field with the density field. We are mainly interested in whether the soliton-like solutions are still

supported by the modified model, and if so, then what their properties would be. The results of numerical experiments performed both for $\sigma < 0$ and $\sigma > 0$ show that, under certain restrictions, the modified model describes the solitary waves of compression and rarefaction, that is, among its solutions, there are the same wave structures as in the model considered in [29]. However, this is where the coincidence of the properties of the models ends, since it is strictly proved in [29] that only solitary waves of rarefaction are spectrally stable under certain conditions, while the solitary waves of compression are always unstable.

The results of current research show that the solitary waves of rarefaction supported by the modified model remain stable. At the same time, previously unstable solitary waves of compression acquire the stability due to the incorporation of the higher order terms of the asymptotic expansion into the dynamic equation of state. It is also shown that an arbitrary initial perturbation in the course of evolution splits into a series of impulses similar to solitary waves of compression, and, thus, some properties of the solutions obtained in the framework of the proposed model coincide with the properties of solutions of completely integrable soliton models. In connection with this, let us note that system (13)–(14) is a modification of model (7)–(8), which does not pass the integrability test [29, 30]. Therefore, system (13)–(14) is most likely nonintegrable as well, but this makes the properties of its solutions even more interesting since they refute to a certain extent the popular belief that the soliton properties of solutions are related to such property of the integrable systems as the presence of an infinite set of conservation laws.

Let us note in conclusion that the presence of soliton solutions in system (13)–(14) is shown in this work using numerical methods. Due to the multidimensionality of the factorized system (16), a strict substantiation of this fact is a rather difficult problem requiring the use of functional methods [21, 25]. For the case of $\sigma < 0$, this problem is solved in the paper [24], but its complete solution, as well as a rigorous proof of the stability of soliton-like solutions in a wide range of parameter's values, requires additional research.

References

1. L. Allen, T. J. Bridges, Hydrodynamic stability of the Ekman boundary layer including interaction with a compliant surface: a numerical framework, *Eur. J. Mech., B, Fluids*, **22**(3): 239–258, 2003, https://doi.org/10.1016/S0997-7546(03)00036-0.

2. L. Allen, T.J. Bridges, Numerical exterior algebra and the compound matrix method, *Numer. Math.*, **92**(2):197–232, 2002, https://doi.org/10.1007/s002110100365.

3. N. Ari, A.C. Eringen, Nonlocal stress field and Griffith crack, *Cryst. Lattice Def. Amorph. Mater.*, **10**:33–38, 1983.

4. B. Barker, J. Humpherys, G. Lyng, J. Lytle, Evans function computation for the stability of travelling waves, *Philos. Trans. R. Soc. Lond., Ser. A, Math. Phys. Eng. Sci.*, **376**(2117): 20170184, 2009, https://doi.org/10.1098/rsta.2017.0184.

5. T.J. Bridges, G. Derks, G. Gottwald, Stability and instability of solitary waves of the fifth-order KdV equation: A numerical framework, *Physica D*, **172**(1–4):190–216, 2002, https://doi.org/10.1016/S0167-2789(02)00655-3.

6. A.R. Champneys, Homoclinic orbits in reversible systems and their applications in mechanics, fluids and optics, *Physica D*, **112**(1–2):158–186, 1998, https://doi.org/10.1016/S0167-2789(97)00209-1.

7. M. Chugunova, D.I. Pelinovsky, Two-pulse solitons in the fifth-order KdV equation: Rigorous theory and numerical approximations, *Discrete Contin. Dyn. Syst., Ser. B*, **8**(4):773–800, 2007, https://doi.org/10.3934/dcdsb.2007.8.773.

8. R.K. Dodd, J.C. Eilbeck, J.D. Gibbon, H.C. Morris, *Solitons and Nonlinear Wave Equations*, Academic Press, London, 1984.

9. A.C. Eringen, Vistas of nonlocal continuum mechanics, *Int. J. Eng. Sci.*, **30**(10):1551–1565, 1992, https://doi.org/10.1016/0020-7225(92)90165-D.

10. J.W. Evans, Nerve axon equations: III Stability of nerve impulse, *Indiana Univ. Math. J.*, **22**(6):577–593, 1972, https://doi.org/10.1512/iumj.1972.22.22048.

11. J.W. Evans, Nerve axon equations: IV The stable and unstable impulse, *Indiana Univ. Math. J.*, **24**(12):1169–1190, 1975, https://doi.org/10.1512/iumj.1975.24.24096.

12. A. Gawlik, V. Vladimirov, S. Skurativskyi, Existence of the solitary wave solutions supported by the modified FitzHugh–Nagumo system, *Nonlinear Anal. Model. Control*, **25**(3):482–501, 2020, https://doi.org/10.15388/namc.2020.25.16842.

13. A. Ghazaryan, S. Lafortune, C.Linhart, Flame propagation in a porous medium, *Physica D*, **413**:132653, 2020, https://doi.org/10.1016/j.physd.2020.132653.

14. A. Ghazaryan, S. Lafortune, V. Manukian, Spectral analysis of fronts in a Marangoni-driven thin liquid film flow down a slope, *SIAM J. Appl. Math.*, **80**(1):95–118, 2020, https://doi.org/10.1137/19M1251977.

15. J. Humpherys, On the shock wave spectrum for isentropic gas dynamics with capillarity, *J. Differ. Equations*, **246**(7):2938–2957, 2009, https://doi.org/10.1016/j.jde.2008.07.028.

16. T. Kapitula, K. Promislov, *Spectral and Dynamical Stability of Nonlinear Waves*, Springer, New York, 2013.

17. V.I. Karpman, Stabilization of soliton instabilities by higher order dispersion: KdV-type equations, *Phys. Lett. A*, **210**:77–84, 1996, https://doi.org/10.1016/0375-9601(95)00752-0.

18. F. Kreten, Traveling waves of an FKPP-type model for self-organized growth, *J. Math. Biol.*, **84**:42, 2022, https://doi.org/10.1007/s00285-022-01753-z.

19. R.H.J. Peerlings, R. de Borst, W.A.M. Brekelmans, J.H.P. de Vree, I. Spee, Some observations on localisation in non-local and gradient damage models, *Eur. J. Mech., A*, **15**:937–953, 1996.

20. R.H.J. Peerlings, M.G.D. Geers, R. de Borst, W.A.M. Brekelmans, A critical comparison of nonlocal and gradient-enhanced softening continua, *Int. J. Solids Struct.*, **38**(44–45):7723–7746, 2001, https://doi.org/10.1016/S0020-7683(01)00087-7.

21. L.A. Peletier, A.I. Rotariu-Bruma, W.C. Troy, Pulse-like spatial patterns described by higher-order model equations, *J. Differ. Equations*, **150**(1):124–187, 1998, https://doi.org/10.1006/jdeq.1998.3480.

22. A.A. Samarsky, Yu.D. Popov, *Difference Schemes for Gasdynamics*, Nauka Publ., Moscow, 1975.

23. B. Sandstede, Stability of travelling waves, in B. Fidler (Ed.), *Handbook of Dynamical Systems, Vol. 2*, Elsevier, Amsterdam, 2002, pp. 983–1055, `https://doi.org/10.1016/S1874-575X(02)80039-X`.

24. L. Sapa, S. Skurativskyi, V. Vladimirov, On the soliton-like solutions of the refined model of elastic media containing inclusions, *Rep. Math. Phys.*, **93**(2):165–177, 2024.

25. D. Smets, J.B. van den Berg, Homoclinic solutions for Swift–Hohenberg and suspension bridge type equations, *J. Differ. Equations*, **184**(1):78–96, 2002, `https://doi.org/10.1006/jdeq.2001.4135`.

26. V.A. Vakhnenko, V.V. Kulich, Long-wave processes in periodic media, *J. Appl. Mech. Tech. Phys.*, **32**:814–820, 1992, `https://doi.org/10.1007/BF00851969`.

27. V.O. Vakhnenko, V.A. Danylenko, A.V. Michtchenko, An asymptotic averaged model of nonlinear long waves propagation in media with a regular structure, *Int. J. Non-Linear Mech.*, **34**(4):643 – 654, 1999, `https://doi.org/10.1016/S0020-7462(98)00014-6`.

28. V.O. Vakhnenko, V.A. Danylenko, A.V. Michtchenko, Diagnostics of the medium structure by long wave of finite amplitude, *Int. J. Non-Linear Mech.*, **35**(6):1105–1113, 2000, `https://doi.org/10.1016/S0020-7462(99)00082-7`.

29. V. Vladimirov, Cz. Maczka, A. Sergyeyev, S. Skurativskyi, Stability and dynamical features of solitary wave solutions for a hydrodynamic-type system taking into account nonlocal effects, *Commun. Nonlinear Sci. Numer. Simul.*, **19**(6):1770–1782, 2014, `https://doi.org/10.1016/j.cnsns.2013.10.027`.

30. V. Vladimirov, S. Skurativskyi, On the spectral stability of soliton-like solutions to a nonlocal hydrodynamic-type model, *Commun. Nonlinear Sci. Numer. Simul.*, **80**:104998, 2020, `https://doi.org/10.1016/j.cnsns.2019.104998`.